Burgers–Rott vortices with surface tension

Yury A. Stepanyants*), Guan H. Yeoh

Reactor Operations, Australian Nuclear Science and Technology Organisation (ANSTO),

Lucas Heights, PMB 1, Menai (Sydney), NSW, 2234, Australia.

*) Corresponding author. Tel.: +61 2 9717 3085; fax: +61 2 9717 9263; e-mail:

Yury.Stepanyants@ansto.gov.au

Summary. A modified Lundgren's model (the LABSRL model) accounting for the effect of surface tension is applied for the description of stationary bathtub vortices in a viscous liquid with a free surface. Laminar liquid flow through the circular bottom orifice is considered in a horizontally unbounded domain with the liquid being assumed to be undisturbed at infinity and approaching to a constant depth. An approximate analytical solution of the LABSRL model is obtained for small-dent vortices. Good agreement is achieved between the constructed analytical and numerical solutions for the same set of parameters.

Keywords. Whirlpool, bathtub vortex, free surface, surface tension, approximate analytical solutions

1. Introduction

Whirlpools or bathtub vortices often appear in bathes, kitchen sinks, laboratory tanks or industrial reservoirs. In spite of their daily occurrences, their structure, formation and subsequent dynamics are still not completely understood and adequately described.

One of the most successful models describing a structure of bathtub vortices in a rotating vessel has been the analytical model proposed by Lundgren [6]. Andersen et al. [1, 2] further extended the model to include the surface tension and bottom upwelling due to viscous effect in the Ekman boundary layer near the outlet orifice. This modified model, designated as the LABSRL model, was verified against the experimental data on whirlpools observation in a rotating cylinder with water circulating at a given flow rate. By adjusting two fitting parameters and solving the resultant set of ordinary differential equations (ODEs) numerically, Andersen et al. [1, 2] obtained good agreement between the theoretical/numerical results and experimental data for moderate flow conditions: drain rate through the vessel, $Q \sim 1.8{\cdot}10^{-6}$ m^3/s, and vessel rotation rate, $\Omega \sim 1.26$ rad/s (~ 12 rpm). The experiments demonstrated that the surface tension significantly affected both the whirlpool shape and its dip, at least when the whirlpool dent was found to be relatively small. In particular, the model without surface tension in one of the cases studied overestimated the depth of experimentally registered whirlpool by 70%, whereas the model with surface tension agreed well with the experimental data.

In the book by Lautrup [5], a model, which bears many similarities with the Lundgren's model, has been derived in describing bathtub vortices in a non-rotating vessel without surface tension. Miles [7], essentially considering the Lundgren–Lautrup model, constructed an approximate solution for the free surface shape caused by a bathtub vortex in the liquid. His solution may well be regarded as an extension of Rott's solution [9] based on the Burgers' vortex theory in viscous fluid [3]. The analytical results from Miles [7] were found to agree rather well with Lundgren's numerical solution [6] in the range of theory validity, i.e. when the whirlpool dip was small in comparison to the total fluid depth.

In our recent work [10], the LABSRL-model with surface tension has been reconsidered for whirlpools in a non-rotating vessel. Basic set of equations was re-examined, derived independently, and studied numerically. The improved LABSRL-model was capable of not only describing the subcritical regime of liquid discharge when whirlpools of small dent appeared on the surface but also critical and even supercritical regimes when the gaseous vortex cores occupied some portion of the bottom outlet orifice. Flow parameters providing the existence of such intense vortices were determined and analysed by neglecting the surface tension. It should be noted that accounting surface tension into the model dramatically increased the complexity of the theoretical and numerical analyses. In [1, 2] and [10], the influence of surface tension was numerically calculated for relatively shallow whirlpools, i.e. for whirlpools of small dents. The motivation for the current study is to further ascertain the important influence of surface tension on whirlpool shapes at least in a first approximation from an analytical perspective. Results obtained through the LABSRL-model with surface tension are presented below.

2. The LABSRL model

Consider a stationary whirlpool and associated surface depression in a liquid discharging from the vessel though the bottom orifice whose radius r_0 is taken to be much smaller in comparison with the vessel radius R_0 (see Fig. 1). The basic set of hydrodynamic equations in cylindrical coordinate system can be presented in dimensionless form (see, e.g., [8, 6, 10]) as:

$$\frac{1}{\xi}\frac{d\left(\xi w_r\right)}{d\xi}+\frac{\partial w_z}{\partial \zeta}=0\,, \tag{1}$$

$$w_r\frac{dw_r}{d\xi}-\frac{w_\varphi^2}{\xi}=-\frac{\partial P}{\partial \xi}+\frac{1}{\mathrm{Re}_g}\frac{d}{d\xi}\left[\frac{1}{\xi}\frac{d\left(\xi w_r\right)}{d\xi}\right], \tag{2}$$

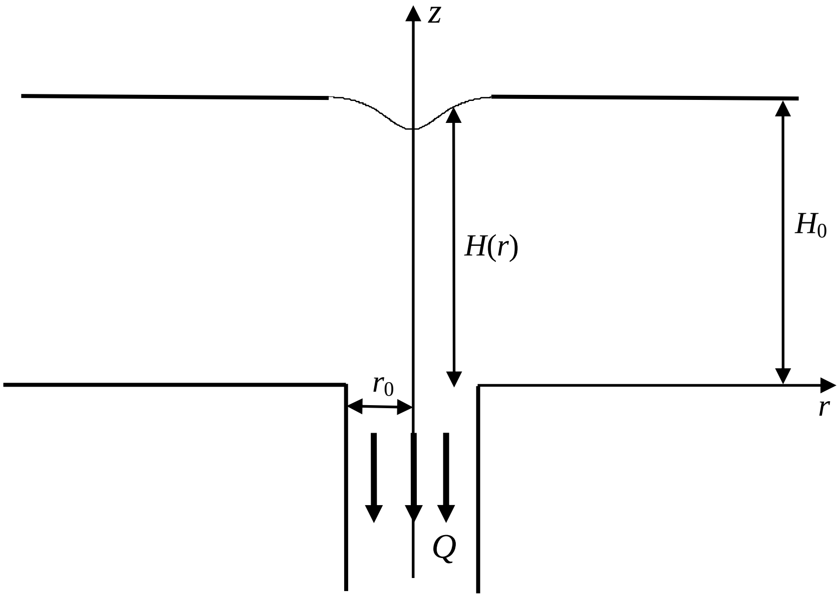

Fig. 1. A schematic drawing of a liquid flow with a small-dent whirlpool in the cylindrical coordinate system. Vessel radius R_0 is not shown in the figure because it is much greater than the radius of the bottom orifice r_0.

$$w_r \frac{dw_\varphi}{d\xi} + \frac{w_r w_\varphi}{\xi} = \frac{1}{\mathrm{Re}_g}\frac{d}{d\xi}\left[\frac{1}{\xi}\frac{d\left(\xi w_\varphi\right)}{d\xi}\right], \tag{3}$$

$$w_r \frac{\partial w_z}{\partial \xi} + w_z \frac{\partial w_z}{\partial \zeta} = -\frac{\partial P}{\partial \zeta} + \frac{1}{\mathrm{Re}_g}\left(\frac{\partial^2 w_z}{\partial \xi^2} + \frac{1}{\xi}\frac{\partial w_z}{\partial \xi} + \frac{\partial^2 w_z}{\partial \zeta^2}\right) - 1, \tag{4}$$

The variables are normalized as:

$$\xi = r/H_0, \quad \zeta = z/H_0, \quad \{w_r, w_\varphi, w_z\} = \{u_r, u_\varphi, u_z\}/U_g, \quad P = p/(\rho U_g^2), \quad \mathrm{Re}_g = H_0 U_g/\nu, \tag{5}$$

where u_r, u_φ and u_z are the components of the velocity field in cylindrical coordinate system, $U_g = (gH_0)^{1/2}$ is the characteristic velocity parameter, H_0 is the unperturbed liquid depth at infinity, ν is liquid kinematic viscosity and Re_g is the “geometric” Reynolds number based on the liquid depth rather than on real fluid velocity.

In the above equations (2) and (4), the pressure field is determined by the formula (for details see [10]):

$$P = P_0 + h(\xi) - \zeta - \frac{\mathrm{We}^{-1}}{\xi}\frac{d}{d\xi}\frac{\xi \frac{dh}{d\xi}}{\sqrt{1+\left(\frac{dh}{d\xi}\right)^2}}\,, \tag{6}$$

where P_0 is the normalized atmospheric pressure, $h(\xi) = H(\xi)/H_0$ is the normalized liquid depth with $H(r)$ being the dimensional liquid depth (see Fig. 1), and the last term represents the normalized pressure due to surface tension with the dimensionless coefficient $\mathrm{We} = \rho U_g^2 H_0 / \sigma = \rho g H_0^2 / \sigma$ being the Weber number; σ is the surface tension coefficient of the gas/liquid interface (cf. [1, 2]).

As shown in [6, 1, 2, 5, 10], this set of hydrodynamic equations can be reduced to the simplified set of ODEs according to:

$$h(\xi)\frac{d}{d\xi}\ln\left[\frac{1}{\xi}\frac{d(\xi w_\varphi)}{d\xi}\right] = -Q_R\xi\begin{cases} 1, & 0 \le \xi \le R; \\ \dfrac{R^2}{\xi^2}, & \xi > R; \end{cases} \tag{7}$$

$$\frac{d}{d\xi}\left[h(\xi) - \frac{\mathrm{We}^{-1}}{\xi}\frac{d}{d\xi}\frac{\xi \frac{dh}{d\xi}}{\sqrt{1+\left(\frac{dh}{d\xi}\right)^2}}\right] = \frac{w_\varphi^2}{\xi}\,, \tag{8}$$

where $R = r_0/H_0$ is the normalized radius of the output orifice and $Q_R = |Q| H_0 / \left(2\pi\nu r_0^2\right) = \left(\mathrm{Re}_g/2\right)\left(U_0/U_g\right)$ is the dimensionless liquid discharge rate with U_0 being the average drainage velocity through the outlet pipe.

These equations are complemented by the boundary conditions at $\xi = 0$:

$$h(0) = h_0, \quad \left.\frac{dh}{d\xi}\right|_{\xi=0} = 0\,, \quad \left.\frac{d^2h}{d\xi^2}\right|_{\xi=0} = h_0''\,, \quad w_\varphi(0) = 0\,, \quad \left.\frac{dw_\varphi}{d\xi}\right|_{\xi=0} = w_\varphi'\,, \tag{9}$$

and at $\xi = \infty$:

$$h(\infty) = 1, \quad \left.\frac{dh}{d\xi}\right|_{\xi=\infty} = 0\,, \quad \left.\frac{d^2h}{d\xi^2}\right|_{\xi=\infty} = 0\,, \quad w_\varphi(\infty) = 0, \quad \left.\frac{dw_\varphi}{d\xi}\right|_{\xi=\infty} = 0\,. \tag{10}$$

There are six parameters altogether characterizing the stationary whirlpool: Q_R, We, R, h_0, h_0'', and w_φ'. For the given values of external parameters which determine the global liquid flow, *viz.*, Q_R, We and R, three other parameters determining the internal whirlpool structure, h_0, h_0'', and w_φ', play a vital role in ascertaining the eigenvalue vector $\boldsymbol{\lambda} = \{h_0,\ h_0'',\ w_\varphi'\}$. Only at certain values of $\boldsymbol{\lambda}$, physically acceptable solutions of the boundary-value problem of equations (7)–(10) can exist. At special conditions, some of the external parameters become appreciably small; the boundary-value problem of equations (7)–(10) can thus be simplified. Numerical solutions of this boundary-value problem were constructed and discussed in [10]. In this paper, we present some results of numerical calculations to validate the analytically constructed approximate solution. For the sake of simplicity, the characteristic vortex radius (which will be precisely defined below) is assumed to be much smaller than the radius of the output orifice, so that the parameter R becomes unimportant. The essential domain of consideration is then $\xi << R$.

3. Approximate analytical solution to the LABSRL model

By assuming that the circulation in the liquid is very small and the depth being sufficiently large, the surface dent caused by the liquid discharge through the bottom outlet can be safely neglected. In this limit, the solution of equations (6) and (7) subject to the boundary conditions (8) and (9) is the so-called Burgers–Rott vortex (see [3, 9, 7]):

$$h(\xi) \approx 1, \qquad w_\varphi(\xi) \approx \frac{\mathrm{K}}{2\pi\xi}\left[1-\exp\left(-\frac{Q_R}{2}\xi^2\right)\right], \tag{11}$$

where $\mathrm{K} = \Gamma/(U_g H_0)$ is the dimensionless Kolf number defined through the average liquid circulation Γ.

The characteristic vortex radius, *i.e.* the coordinate where the azimuthal velocity maximum occurs is: $\xi_c \equiv r_c/H_0 = \sqrt{2\vartheta/Q_R}$, where $\vartheta \approx 1.256$ is the root of the transcendental equation $2\vartheta = e^{\vartheta} - 1$. The maximum value of azimuthal velocity is:

$$\left(w_\varphi\right)_{\max} \equiv w_\varphi\left(\xi_c\right) = \frac{\mathrm{K}\sqrt{Q_R}}{2\pi\Theta}, \quad \Theta = \frac{\sqrt{2\vartheta}}{1-\mathrm{e}^{-\vartheta}} \approx 2.216. \tag{12}$$

Carrying out the transformation whereby $x = Q_R^{1/2}\xi$ and $\upsilon = w_\varphi / \left(w_\varphi\right)_{\max}$ and denoting $\varepsilon = \left(w_\varphi\right)_{\max}^2$ and $\mu = Q_R/\mathrm{We}$, equations (7) and (8) can be expressed in terms of the new variables as:

$$h(x)\frac{d}{dx}\ln\left[\frac{1}{x}\frac{d(x\upsilon)}{dx}\right] = -x, \tag{13}$$

$$\frac{d}{dx}\left[h(x) - \frac{\mu}{x}\frac{d}{dx}\frac{x\,\frac{dh}{dx}}{\sqrt{1+Q_R\left(\frac{dh}{d\xi}\right)^2}}\right] = \varepsilon\,\frac{\upsilon^2}{x}. \tag{14}$$

When μ = 0, this set of equations is equivalent to that considered by Miles [7] who constructed an approximate analytical solution for the whirlpool shape assuming the parameter $\varepsilon << 1$. Accordingly, both parameters ε and μ are assumed to be small but finite as well as the hierarchical condition of $\varepsilon << \mu << 1$ prevails. These inequalities in the dimensional variables is equivalent to the following relationship between physical parameters: $\rho\Gamma^2/(H_0\sigma) \ll (2\pi\Theta)^2 \approx 193.87$ and $\sigma U_0/(H_0\rho g \nu) \ll 2$. For water whirlpools, these conditions reduce particularly to $\Gamma \ll 0.118\sqrt{H_0}$ m^2/s and $U_0 \ll 0.243 H_0$ m/s.

Expressing a solution to the set of equations (13) and (14) in the form of Taylor series in the parameters ε and μ, it can be shown that in the leading order the series are given as:

$$h(x) = 1 + \varepsilon h_1(x) + \varepsilon\mu h_2(x) + \dots, \quad \upsilon(x) = \upsilon_0(x) + \varepsilon\upsilon_1(x) + \varepsilon\mu\upsilon_2(x) + \dots, \tag{15}$$

where $\upsilon_0(x)$ is the zero-order solution (11) for the azimuthal velocity in new variables, *viz*, $\upsilon_0(x) = \Theta\left(1 - e^{-x^2/2}\right)/x$, and $h_i(x)$ and $\upsilon_i(x)$ are the first-, second-, and higher-order corrections. Substitution these series into equations (13) and (14) yields the equations for the first-order corrections to functions $h(x)$ and $\upsilon(x)$ on the parameter ε only:

$$\frac{dh_1}{dx} = \frac{\upsilon_0^2}{x}, \tag{16}$$

$$\frac{d}{dx}\left[\frac{1}{x}\frac{d(x\upsilon_1)}{dx} + x\upsilon_1\right] = -h_1\frac{d}{dx}\left[\frac{1}{x}\frac{d(x\upsilon_0)}{dx}\right]. \tag{17}$$

Integration of the above equations subject to the boundary conditions (9) and (10) results in the following expression for the liquid surface (cf. [7]):

$$h_1(x)=\frac{\Theta^2}{2}\left[\mathrm{E}_1\left(x^2\right)-\mathrm{E}_1\left(x^2/2\right)-\left(\frac{1-e^{-x^2/2}}{x}\right)^2\right], \tag{18}$$

where $\mathrm{E}_1(x)\equiv-\mathrm{Ei}(-x)=\int_x^\infty \frac{e^{-u}}{u}du$, is the exponential integral (see, e.g., the website [12]).

The first-order correction to the azimuthal velocity component is described by the following equation:

$$\frac{d}{dx}\left[\frac{1}{x}\frac{d\left(x\upsilon_1\right)}{dx}+x\upsilon_1\right]=-h_1\frac{d}{dx}\left[\frac{1}{x}\frac{d\left(x\upsilon_0\right)}{dx}\right]. \tag{19}$$

Integrating this equation yields

$$\upsilon_1(x)=\frac{\Theta^3}{4x}\left\{\mathrm{E}_1\left(x^2/2\right)-4\mathrm{E}_1\left(x^2\right)+3\mathrm{E}_1\left(3x^2/2\right)+\left(1-e^{-x^2/2}\right)\ln\frac{27}{64}+\right.$$
$$\left.e^{-x^2/2}\left[x^2\left\{\mathrm{E}_1\left(x^2/2\right)-\mathrm{E}_1\left(x^2\right)\right\}+\left(1-e^{-x^2/2}\right)^2+4\mathrm{E}_1\left(x^2/2\right)-3\mathrm{E}_1\left(x^2\right)+\ln\frac{27x^2}{256}+C_{EM}\right]\right\}, \tag{20}$$

where $C_{\mathrm{EM}}\approx 0.5772$, which is the Euler–Mascheroni constant.

Essentially, the same solutions for the first-order corrections have been obtained by Miles [7]. The expression for the velocity correction, $\upsilon_1(x)$, is however left in the quadrature form in his derivation. As shown from above, the corresponding integrals may be calculated in close analytical forms and the result can be presented in terms of the same transcendential function $\mathrm{E}_1(x)$ as in the correction to the vortex shape.

The equations for the second-order corrections $h_2(x)$ and $\upsilon_2(x)$ are:

$$h_2(x) = \frac{1}{x}\frac{d}{dx}\left(\frac{\upsilon_0^2}{\sqrt{1+\varepsilon^2 Q_R\,\upsilon_0^4/x^2}}\right), \tag{21}$$

$$\frac{d}{dx}\left[\frac{1}{x}\frac{d(x\upsilon_2)}{dx} + x\upsilon_2\right] = -2\frac{\upsilon_0}{x}\frac{d\upsilon_0}{dx}\frac{d}{dx}\left[\frac{1}{x}\frac{d(x\upsilon_0)}{dx}\right] = 2\Theta^3\frac{1-e^{-x^2/2}}{x^3}e^{-x^2/2}\left[\left(x^2+1\right)e^{-x^2/2}-1\right], \tag{22}$$

and their solutions are:

$$h_2(x) = 2\Theta^2\frac{1-e^{-x^2/2}}{x^4}\left\{\frac{x^2e^{-x^2/2}-1+e^{-x^2/2}}{\sqrt{1+\varepsilon^2 Q_R\Theta^4\left(1-e^{-x^2/2}\right)^4/x^6}} - \varepsilon^2 Q_R\Theta^4\frac{\left[x^2e^{-x^2/2}-\frac{3}{2}\left(1-e^{-x^2/2}\right)\right]\left(1-e^{-x^2/2}\right)^4/x^6}{\left[1+\varepsilon^2 Q_R\Theta^4\left(1-e^{-x^2/2}\right)^4/x^6\right]^{3/2}}\right\}, \tag{23}$$

$$\upsilon_2(x) = \frac{\Theta^3}{2x}\left[2\mathrm{E}_1\left(x^2\right) - \mathrm{E}_1\left(x^2/2\right) - \mathrm{E}_1\left(3x^2/2\right) - \ln\frac{3}{4}\right]. \tag{24}$$

Hence, the first-order corrections to the Burgers–Rott vortex due to gravity and surface tension effects can be presented through the approximate solutions to the LABSRL model in the form of Taylor series of equation (15) with equations (18), (20), (23) and (24) for the corresponding terms. Asymptotic representation of this solution in the vicinity of $x = 0$ is:

$$h(x) \approx 1 + \frac{\varepsilon\Theta^2}{2}\left\{-\ln 2 + \frac{x^2}{4} - \frac{x^4}{16} + \mu\left[1 - \left(1 + \frac{\Theta^4}{16}\varepsilon^2 Q_R\right)x^2 + \left(1 + \frac{9\Theta^4}{28}\varepsilon^2 Q_R + \frac{9\Theta^8}{896}\varepsilon^4 Q_R^2\right)\frac{7x^4}{16}\right]\right\} + O\left(x^6\right), \tag{25}$$

$$\upsilon(x) \approx \frac{\Theta}{2}\left[x - \frac{x^3}{4} + \frac{x^5}{24} + \frac{\varepsilon\Theta^2}{2}x^3\left(-\ln 2 + \frac{\mu}{4} + \frac{1+4\ln 2 - 2\mu}{12}x^2\right)\right] + O\left(x^7\right). \tag{26}$$

It is observed from equation (25) that the minimum value of $h(x)$ occurs at $x = 0$ and equals to

$$h(x) \approx 1 + \varepsilon\Theta^2\left(-\frac{\ln 2}{2} + \mu\right) = 1 + \frac{Q_R \mathrm{K}^2}{4\pi^2}\left(-\frac{\ln 2}{2} + \frac{Q_R}{\mathrm{We}}\right). \tag{27}$$

Therefore, the surface tension correction, proportional to μ, always acts in the direction of diminishing of whirlpool dip. This agrees well with the physical expectation and results of experimental observations [1, 2] and numerical modeling [10].

Note that solution (23) contains terms of the order of ε^2, but only in a combination with Q_R. The last parameter can be taken to be substantially large, so that the combination $\varepsilon^2 Q_R$ may not be negligible. Moreover, it can even be much greater than unity. In the last case, the characteristic scale of the second-order correction, $h_2(x)$, becomes $x_\mu = 4/(\Theta^2 \varepsilon Q_R^{1/2})$; it is of the order of unity if $\varepsilon^2 Q_R \Theta^4 << 1$.

In the limit of small x, the corrections to the azimuthal velocity both of the first- and second-order are proportional to x^3. For small values of ε and μ, the corrections are very small in reality. Hence, the Burgers formula for the vortex velocity $\upsilon_0(x)$ [3] is a good approximation of the azimuthal velocity component in a real whirlpool velocity field, at least when the whirlpool dip is relatively small in comparison with the total liquid depth.

The solution obtained is shown in Fig. 2 for $\varepsilon = 0.0171$ and three values of μ: $\mu = 0$ (no surface tension), $\mu = 0.0564$ and $\mu = 0.1647$. It is evidenced that the whirlpool dip diminishes due to the effect of surface tension. Its curvature at $x = 0$ decreases as μ increases:

$$Cur(0) = \frac{\varepsilon\Theta^2}{4}\left\{1 - 4\mu\left[1 + Q_R\left(\frac{\varepsilon\Theta^2}{4}\right)^2\right]\right\}. \tag{28}$$

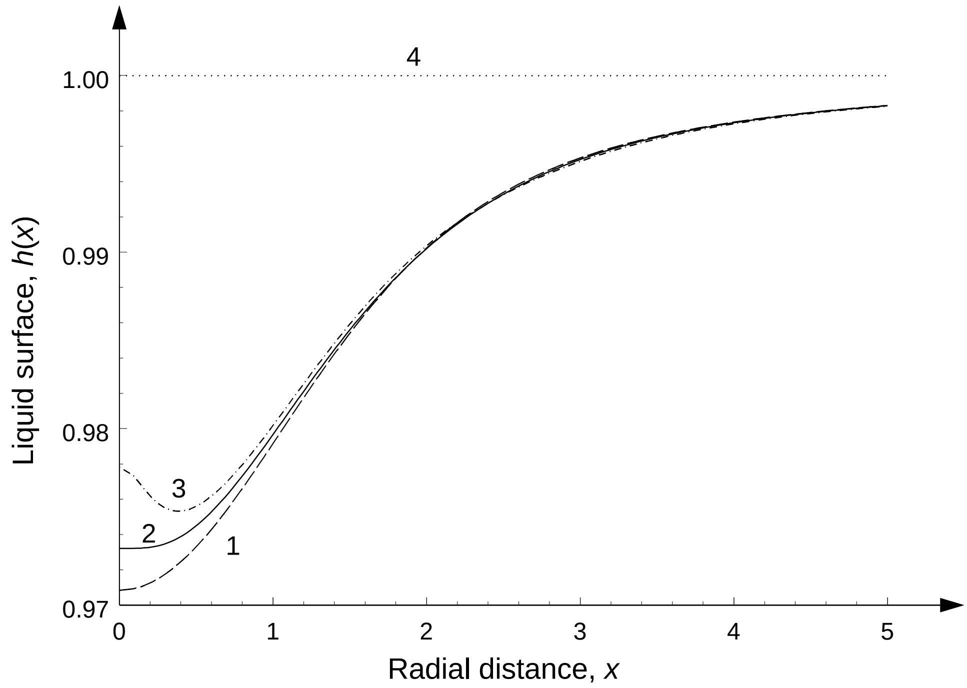

a)

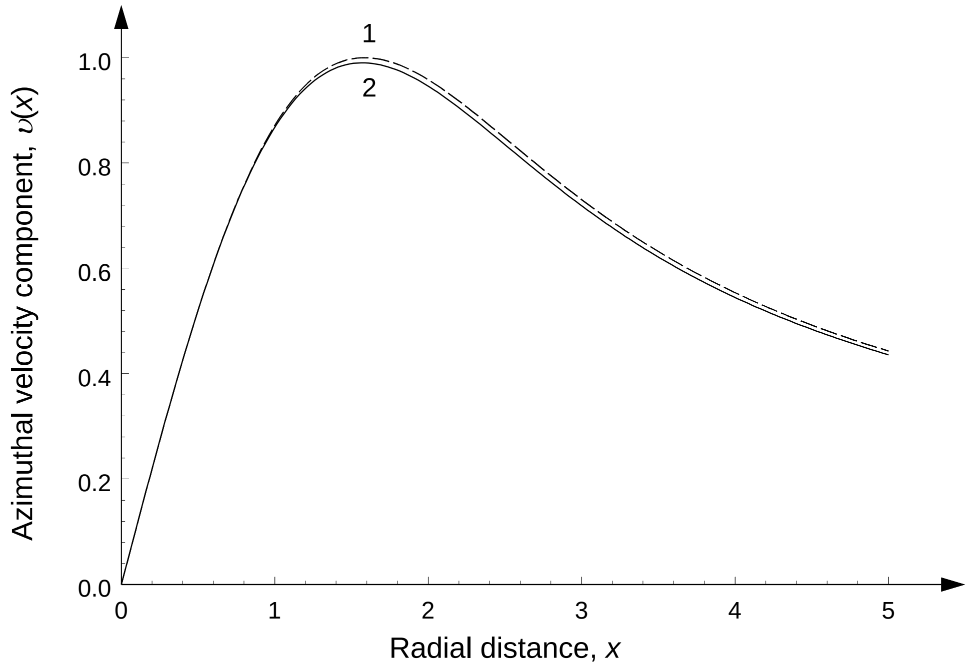

b)

Fig. 2. a) – Vortex profile versus dimensionless radial coordinate x for $\varepsilon = 0.0171$ and three values of μ: $\mu = 0$ ($Q_R = 7.67 \cdot 10^3$) – dashed line 1 (no surface tension), $\mu = 0.0564$ ($Q_R = 7.67 \cdot 10^3$) – solid line 2, and $\mu = 0.1647$ ($Q_R = 2.24 \cdot 10^4$) – dashed-dotted line 3. Dotted line 4 shows unperturbed liquid surface position. b) – azimuthal velocity component versus radial coordinate for $\varepsilon = \mu = 0$ (the Burgers vortex) – dashed line 1 and for $\varepsilon = 0.0171$, $\mu = 0.1647$ – solid line 2. (For better resolution only fragments of plots are shown in the range $0 \le x \le 5$.).

Moreover, the curvature becomes negative when $\mu > 0.25 \big/ \left(1 + \varepsilon^2 Q_R \Theta^4 / 16\right)$. In such a case, a small narrow hump forms in the centre of the vortex dent (see line 3 in Fig. 2a). A similar effect of the hump formation was also obtained in the numerical study of liquid outflow from cylindrical vessel [4, 11]. It was found in particular that the hump may reach the unperturbed free-surface level [4]. However, such solutions in both papers [4, 11] have been obtained for the case of an irrotational liquid discharge within the framework of the potential theory with the surface tension being neglected. The hump formation in our case though looks outwardly similar at this juncture but is rather different from those in [4, 11]. The physical cause of hump formation in all cases, apparently, is related to the fast convergence of the velocity field to the vertical axis; this has been demonstrated by Zhou & Graebel in [11]. The phenomenon requires further investigation in order to better understand the process of liquid discharge from the vessels with and without surface tension, as well as with and without circulation.

The azimuthal velocity is shown in Fig. 2b for the case of $\mu = 0.1647$. The corrections to the Burgers velocity profile are very small even for relatively large value of μ.

4. Comparison of approximate analytical solution with numerical calculations

To validate the constructed approximate solution, the set of ODEs (11)–(12) was solved numerically subject to the corresponding boundary conditions of equations (9) and (10) in the new dimensionless variables. The main difficulty with the numerical solution of this boundary-value problem lies pre-dominantly in determining the appropriate values for the eigenvalue vector $\boldsymbol{\lambda} = \{h_0,\ h_0'',\ \upsilon'\}$, which essentially contains three unknown parameters for a given set of external parameters ε, μ and Q_R. The constructed approximate solution from the above nonetheless significantly assists in the choice of at least one of three unknown parameters, *viz*., υ'.

As follows from the approximate solution, the velocity gradient, υ', at $x = 0$ is unaffected by the first- and second-order corrections and can thus be taken from the Burgers zero-order solution $\upsilon_0(x)$. Two other parameters, h_0 and h_0'', can also been estimated rather accurately from the approximate solution. Our calculations have shown that the value of liquid depth in the whirlpool centre, h_0, was given by the approximate solution fairly precisely, whereas the whirlpool curvature at the centre, h_0'', being actually only the unknown eigenvalue parameter, was easily determined in the course of computations with the starting value taken from the approximate solution of equation (27).

Results of calculations with the same parameters as in Fig. 2 are shown in Fig. 3 for the whirlpool profile (line 1 – approximate theoretical solution, dotted line 2 – numerical solution).

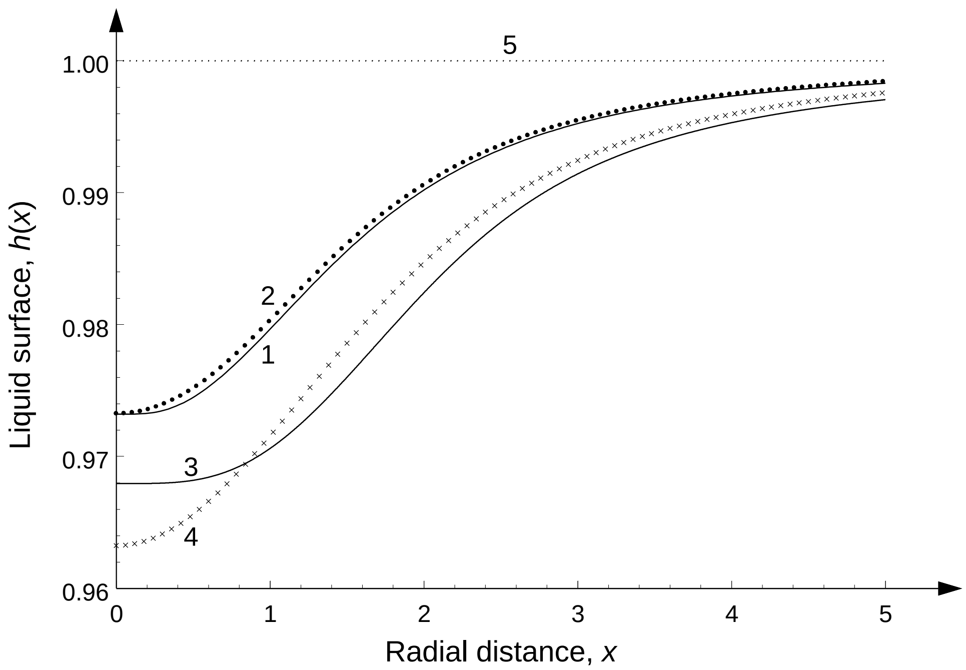

Fig. 3. Analytical versus numerical solutions for the vortex profile. Case 1: ε = 0.0171, μ = 0.0564, Q_R = 7.67·10^3, solid line 1 – approximate analytical solution, dotted line 2 – numerical solution. Case 2: ε = 0.0576, μ = 0.24, Q_R = 8.33, solid line 3 – approximate analytical solution, crossed line 4 – numerical solution. Dotted line 5 shows unperturbed liquid surface position.

The numerical solution has been obtained with parameters $h_0 \approx 0.973$ and $\upsilon' \approx 1.11$ taken from the theoretical prediction. The value of whirlpool curvature at x = 0 was found numerically to be about 60 times greater than the theoretically predicted value: $h_0'' \approx 2.56 \cdot 10^{-4}$. Calculations showed that the solution behavior at the right end of the integration interval (in our case x_{end} = 10) was very sensitive to the choice of the parameter h_0'' value at the left end of the interval, x = 0. The correct solutions were obtained with considerable fine tuning of that parameter.

Values of external dimensionless parameters ε, μ and Q_R used in this example corresponded to the water discharge at room temperature 25°C from the cylindrical vessel of 1 m depth. Drainage velocity was taken as $U = 5{\cdot}10^{-3}$ m/s, water density ρ = 997.1 kg/m^3, kinematic viscosity $\nu = 8.94{\cdot}10^{-7}$ m^2/s, surface tension $\sigma = 7.2{\cdot}10^{-2}$ N/m, circulation $\Gamma = 6.52{\cdot}10^{-2}$ m^2/s. The depth of the whirlpool dent for such set of parameters is η = 2.67 cm and whirlpool characteristic radius is r_c = 1.81 cm.

As expected, good quantitative agreement between the approximate analytical and numerical solutions occurred when parameters ε and μ were small and taken in accordance with the assumption $\varepsilon \ll \mu \ll 1$. To assess the robustness of the constructed approximate solution when this assumption was violated, the analytical solution for fairly large values of $\varepsilon = 5.76{\cdot}10^{-2}$ and μ = 0.24 was obtained and plotted in Fig. 3 (solid line 3) against the numerical solution (crossed line 4) for the same external parameters ε, μ and Q_R = 8.33. A quantitative difference between these two solutions can be clearly seen from Fig. 3. The differences between the theoretical and numerical whirlpool parameters were: $(h_0)_{theor}$ = 0.96796, $(h_0)_{num}$ = 0.96324; $(h_0'')_{theor}$ = 0, $(h_0'')_{num}$ = 0.01994; $(\upsilon')_{theor}$ = 1.108, $(\upsilon')_{num}$ = 0.7756. In spite of these differences, vortex profiles (lines 3 and 4) qualitatively agree rather well with each other. Theoretical values imposed for the internal eigenvalue parameters were found to be useful in attaining the numerical solution.

5. Conclusion

An approximate analytical solution has been derived from the basic LABSRL model describing stationary whirlpools on a surface of viscous liquid flowing out of a container through the bottom orifice. The model is a generalization of the Lundgren model [6] pertaining to the case when the surface tension is not negligible. Such extension has been previously suggested in [1, 2] for a liquid in a rotating tank. The solution to the LABSRL model constructed here also accounts for in the first approximation of the surface tension effect, and reduces to the approximate solution ascertained by Miles [7] when the surface tension is neglected. The range of applicability of the approximate solution is restricted by relatively small discharge velocities and circulations. Consequently, the solution only describes whirlpools of relatively small dent depths.

Theoretical results have been validated by direct numerical calculations. Good agreement was achieved between approximate analytical and numerical solutions for the same set of parameters within the range of theory validity. Meanwhile, the approximate solution assisted in solving the basic boundary value problem for vortex shape and velocity and provided the means of obtaining suitable starting values for the three component of the unknown eigenvalue vector. This has allowed us to construct numerical solutions even beyond the range of validity of the approximate theory.

References

1. A. Andersen, T. Bohr, B. Stenum, J.J. Rasmussen and B. Lautrup, Anatomy of a bathtub vortex, *Phys. Rev. Lett.*, **91** (2003) 104502, 4 p.
2. A. Andersen, T. Bohr, B. Stenum, J.J. Rasmussen and B. Lautrup, The bathtub vortex in a rotating container, *J. Fluid Mech.*, **556** (2006) 121–146.
3. J.M. Burgers, A mathematical model illustrating the theory of turbulence, *Advances in Applied Mechanics* (Academic Press, New York 1948), vol. 1, pp. 171–199.
4. L.K. Forbes and G.C. Hocking, The bath-plug vortex, *J. Fluid Mech.*, **284** (1995) 43–62.
5. B. Lautrup, *Physics of Continuous Matter: Exotic and Everyday Phenomena in the Macroscopic World*, IoP Publishing Ltd, Bristol and Philadelphia 2005, 608 p.

6. T.S. Lundgren, The vertical flow above the drain-hole in a rotating vessel, *J. Fluid Mech.*, **155** (1985) 381–412.
7. J. Miles, A note on the Burgers–Rott vortex with a free surface, *J. Appl Math. Phys. (ZAMP)* **49** (1998) 162–165.
8. A.J. Odgaard, Free-surface air core vortex, *J. Hydr. Eng.*, **112** (1986) 610–620. (See also a discussion on this paper: J.S. Gulliver, T.C. Paul and A.J. Odgaard, J. Hydr. Eng., **114** (1988) 447–452.)
9. N. Rott, On the viscous core of a line vortex, *J. Appl Math. Phys. (ZAMP)* **9b** (1958) 543–553.
10. Y.A. Stepanyants and G.H. Yeoh, Stationary bathtub vortices and a critical regime of liquid discharge, *J. Fluid Mech.*, (2008) to be published.
11. Q.-N. Zhou and W.P. Grabel, Axisymmetric drainage of a cylindrical tank with a free surface. *J. Fluid Mech.*, **221** (1990) 511–532.
12. Website: http://mathworld.wolfram.com/ExponentialIntegral.html